The Surface of Imidazolium-Based Ionic Liquids Consists of Two Interfaces

Helga Tóth Ugyonka,[1] György Hantal,[2] István Szilágyi,[3] Abdenacer Idrissi,[4] Miguel Jorge,[5] and Pál Jedlovszky[1*]

[1]*Department of Chemistry, Eszterházy Károly Catholic University, Leányka utca 12, H-3300 Eger, Hungary*

[2]*PULS Group, Department of Physics, Friedrich-Alexander-Universität Erlangen-Nürnberg, Cauerstr. 3, D-91058 Erlangen, Germany*

[3]*MTA-SZTE Lendület Biocolloids Research Group, Department of Physical Chemistry and Materials Science, Interdisciplinary Excellence Center, University of Szeged, H-6720 Szeged, Hungary*

[4]*University of Lille, CNRS UMR 8516 -LASIRe - Laboratoire Avancé de Spectroscopie pour les Interactions la Réactivité et l'environnement, 59000 Lille, France*

[5]*Department of Chemical and Process Engineering, University of Strathclyde, 75 Montrose Street, Glasgow G1 1XJ, United Kingdom*

Abstract:

Room temperature ionic liquids (RTILs) are important in a myriad of applications and exhibit fascinating properties arising from a delicate interplay between their ionic and apolar groups. Here, using molecular simulations coupled with intrinsic surface analysis, we reveal how this interplay is responsible for the unique properties of the RTIL surface. Our results show that this surface can be viewed as a superposition of two "interfaces", one between a hydrophobic layer of cation alkyl chains and the vapor phase, and another between that hydrophobic layer and an ionic fluid composed of polar groups of the cations and anions. Remarkably, the properties of this ionic surface are practically independent of the cation alkyl chain length, suggesting they are a universal feature of imidazolium-based RTILs. This finding has potential implications in the selection and design of RTIL systems for separation applications, which depend on interactions between penetrant molecules and the RTIL surface.

***e-mail:** jedlovszky.pal@uni-eszterhazy.hu (P.J.)

This is a peer-reviewed, accepted manuscript of the following paper: Tóth Ugyonka, H., Hantal, G., Szilágyi, I., Idrissi, A., Jorge, M., & Jedlovszky, P. (in press). The surface of imidazolium-based ionic liquids consists of two interfaces. The Journal of Physical Chemistry Letters.

Room temperature ionic liquids (RTILs) are widely used in many fields of chemistry and chemical technology, from synthesis[1] to catalysis,[2] electrochemistry,[3,4] or gas capture.[5-7] Many of these applications involve the surface of these liquids; however, considerably less attention has been paid so far to the interfacial properties of RTILs than to their bulk ones. Nevertheless, several experimental[8-13] and simulation[14-26] investigations, including advanced simulation methodologies, such as metadynamics[27-29] of the liquid-vapor[8-26] and liquid-solid interfaces[27-29] of RTILs, particularly for imidazolium-based systems, were reported in the past two decades. The general picture emerging from these studies is that the free surface of imidazolium-based RTILs contains excess amount of cations, and the cation hydrocarbon chains turn preferentially toward the vapor phase.

It should be emphasized that the surface of fluid phases is corrugated, on the molecular length scale, by thermal capillary waves,[30] and thus, when analyzing the surface properties at the molecular level, the smearing effect of these capillary waves needs to be removed (in other words, the full list of particles that stay right at the boundary of the two phases is needed to be determined). Since the pioneering work of Chacón and Tarazona more than two decades ago,[31] a number of methods capable of doing this task have been developed,[32-37] among which the **i**dentification of the **t**ruly **i**nterfacial **m**olecules (ITIM)[34] turned out to be an excellent tradeoff between computational cost and accuracy.[35] It has also been repeatedly shown that the neglect of the effect of the capillary waves leads to a systematic error of unknown magnitude in the calculated structural,[16-18,20,25,33-35] dynamical,[17,20,26] and even thermodynamic properties.[38] Further, performing intrinsic surface analysis was found to be inevitable in explaining several experimental findings, such as the surface tension anomaly of water.[39,40]

Recently, we demonstrated by the combination of computer simulation and intrinsic surface analysis done at atomistic rather than molecular resolution that, in spite of this excess amount of cations, the RTIL surface bears a small negative charge, which is already compensated in the subsequent one or two atomic layers.[25] The physical reason behind this negative surface charge is that the hydrocarbon chains, staying preferentially at the liquid surface, carry no charge, but effectively shield charged moieties of the cations from the vapor phase, while the smaller and more mobile anions can somewhat penetrate among these chains.[25] These structural peculiarities largely determine also the dynamics of the liquid surface.[26] It should be noted that a negative surface charge of imidazolium-based RTILs was already suggested by Sloutskin et al. in interpreting their X-ray reflectivity experiments.[9] This finding naturally raises the question of how the cation alkyl chain length influences the

interfacial structure. Our hypothesis, which we set out to test in this paper, is that the RTIL liquid surface can be interpreted as the combination of two consecutive "interfaces": an outer liquid-vapor interface between the hydrocarbon layer and the vapor, and an inner one akin to a liquid-liquid interface between the ionic moieties and the hydrocarbon layer (see Figure 1). We then test how the atomistic structure of the interface beneath this outer hydrocarbon layer depends on the alkyl chain length.

To address this question, we performed computer simulations of the liquid-vapor interface of three imidazolium-based RTILs, consisting of 1-alkyl-3-methylimidazolium cations and PF_6^- anions, differing solely in the alkyl chain length. This chain was chosen to be 1, 4, and 8 carbon atoms long (i.e., methyl, butyl, and octyl), corresponding to [mmim][PF_6], [bmim][PF_6], and [omim][PF_6], respectively. The structure of these ions is shown in Figure S1 of SI. To remove the smearing effect of thermal capillary waves,[30] we determined the real, atomistically corrugated intrinsic surface using the ITIM method,[32] by disregarding the atoms pertaining to the last 3 and 7 CH_2/CH_3 groups of the chains of the $bmim^+$ and $omim^+$ cations, respectively, from the determination of the intrinsic surface. The ITIM analysis performed this way therefore provides information about the *atoms pertaining to the surface beneath the hydrocarbon layer that covers the liquid*. To distinguish this surface, which marks the interface between the ionic groups and the surface hydrocarbon layer, from the true surface of the liquid phase, the former is referred to here as the 'ionic surface' of the liquid. It should be noted that for [mmim][PF_6], lacking the apolar alkyl chain, it strictly coincides with the real liquid surface. ITIM analyses are done atomistically, i.e., it is decided for each atom individually whether it pertains to the surface layer or not. For reference, ITIM analysis is repeated in molecular resolution, i.e., the entire ion is considered as belonging to the surface layer if any of its atoms is found to be at the surface.[25]

Simulations have been done in the canonical (N,V,T) ensemble with 864 ion pairs, using the GROMACS 2019.3 software,[41] as described in our previous publications.[25,26] Both [bmim][PF_6] and [omim][PF_6] have been simulated at two different temperatures, i.e., 298 K and 398 K, while [mmim][PF_6], being solid at 298 K, has only been simulated at 398 K. Ions have been described by the OPLS-based[42] scaled-charge potential model of Doherty et al.[43] This model was shown to well reproduce the experimental values of density, heat capacity, self-diffusion coefficient, viscosity, heat of vaporization, and interfacial tension for a large number of imidazolium-based RTILs.[43] In particular, it captures the heat of vaporization and surface tension, i.e., thermodynamic quantities related to the coexisting liquid and vapour phases, typically within 1-2% for imidazolium-based RTILs consisting of the PF_6^- anion.[43] All

interactions have been truncated to zero beyond the center-based cut-off of 13 Å; the long range part of both the electrostatic and the Lennard-Jones interaction has been accounted for by the particle mesh Ewald (PME) method.[44,45] Temperature has been controlled by the v-rescale thermostat.[46] Following an equilibration period of at least 0.1 μs, 20000 sample configurations have been dumped for the analyses from the 0.1 μs long production run for each system. ITIM analyses have been performed using the freely available[47] Pytim software,[48] employing a probe radius of 2 Å and grid spacing of 0.4 Å.[25]

We start by analyzing the layerwise molecular structure[49] of the ionic surface. The mole fraction of the cations in the first four molecular layers beneath the ionic surface is shown in Figure 2.a. This profile does not show marked variation with either the temperature or the alkyl chain length – differences between systems at the same temperature is typically ~1-2%, and never exceeds 7%. For comparison, at the real liquid surface (accessed using the "standard" ITIM procedure, i.e. considering also the alkyl chains), these differences are ~20-40% (see Fig.2.b).

The composition of the atomic layers beneath the ionic surface also exhibits remarkable similarities between different systems at both temperatures (see Figure 3.a). The only marked difference arises from the trivial fact that the two methyl groups of the $mmim^+$ cation are equivalent, while this is clearly not the case for the larger cations. Hence, the mole fraction of the methyl group atoms in [mmim][PF_6] is roughly the average of those of the methyl and alkyl trunk CH_2 groups in [bmim][PF_6] and [omim][PF_6] in each layer. Again, no such similarity in the composition of the surface atomic layers is seen at all, if the real liquid surface is considered (see Figure S2 of SI).

The similar composition of the atomic layers beneath the ionic surface implies that they are characterized by similar charge (surface) densities in different systems, as shown in the top panel of Fig. 3.b. The first atomic layer at the ionic surface has a roughly -3.5×10^{-3}e/Å^2 charge surface density, which is already largely compensated in the second layer. By contrast, the charge density distributions in layers beneath the real liquid surface show no such similarities (see the bottom panel of Fig. 3.b).

All these results imply that the atomistic structure of the ionic surface is strikingly similar for all of the studied RTILs and, hence, it is largely independent from the chain length of the cations. By implication, we can conclude that the differences observed when the real liquid surface is considered as a reference arise primarily from the different extents of coverage of the ionic surface by the hydrophobic layer of cation alkyl chains. Such an increase in the coverage of the surface by non-polar groups has been previously demonstrated

both by experimental[9,13,50-52] and computer simulation studies.[15-18] Nevertheless, all layerwise profiles shown in Figs. 2 and 3 exhibit some residual differences between different RTILs. To investigate whether these differences are caused by the different cation chain lengths or are instead due to statistical uncertainties, we have calculated the density profiles of several atoms (Figure 4), as well as the charge density profile and its cation/anion contributions (Figure 5). All profiles were calculated with respect to the intrinsic ionic surface, thus X_{intr}=0 marks the position of the surface itself, whereas negative and positive X_{intr} values correspond to the ionic liquid and hydrocarbon regions, respectively.

Before interpreting these profiles, two remarks are in order. First, since the intrinsic surface is defined by the outermost layer of atoms, their distance from the intrinsic surface is zero by definition, yielding a Dirac delta peak at X_{intr}=0Å; hence, the continuous part of the profiles describes the structure *from the second layer on*.[35,49] Second, the profiles reflect the trivial fact that the bulk density of the *ionic groups* decreases with increasing alkyl chain length (i.e. longer chains occupy larger volume). This difference is not specific to the surface but affects also the bulk liquid; therefore, density profiles obtained in different systems reach different limiting values upon approaching the bulk liquid phase (see Figures S3 and S4 of SI). To emphasize the real structural differences between the ionic surface of different systems, all profiles were normalized by the corresponding bulk phase value, estimated by averaging the corresponding profiles in the -30Å $\leq X_{intr} \leq$ -25Å range.

Figs. 4 and 5 reveal that, despite their general similarities, the profiles obtained in different systems also exhibit some small differences, particularly in the X_{intr} range of their first continuous peak (corresponding to the second atomic layer). This peak is typically higher in the presence of cations with shorter alkyl chain. In other words, the structure of the profiles in this region is progressively washed out with increasing alkyl chain length. We have ruled out the possibility that this effect is due to an increase in the number of ionic moieties "dissolved" in the outermost hydrocarbon layer as it becomes wider, by repeating the ITIM analysis for [omim][PF_6] at 398K while filtering out these 'dissolved' ionic moieties using the DBSCAN method[53] (see Figure 6.a).

The other possibility is that a difference in the chain length modifies the strength of certain orientational preferences of the imidazolium ring at the ionic surface. Similar effect was found earlier at the real liquid surface.[18] Alkyl chain-induced differences in the orientational distribution of the rings can readily explain the observed small differences between the ionic surface structures of different systems. To test this possibility, we have calculated the cosine distribution of the angle between the vector joining the two N atoms of

the ring (referred to as the **NN** vector, see Fig. S1 of SI) and the surface normal vector, **X**, directed to point away from the ionic liquid phase. The distribution obtained in the first molecular layer is compared at 398K for the different systems in Fig. 6.b. The distributions have their main maximum at cosγ=1 (chains pointing to the vapor) and another, smaller one at cosγ=-1 (chains pointing to the liquid), in accordance with earlier findings.[16,18] The former peak becomes lower, while the latter becomes higher with decreasing chain length, indicating weakening and strengthening of the respective orientational preferences. Further, the probability of observing rings oriented parallel to the surface (cosγ=0) also decreases with increasing chain length. Both effects contribute to "push" ionic moieties further towards the bulk region as the alkyl chain length increases, in qualitative agreement with experimental observations,[54] which can explain the small differences in the profiles shown in Figs. 4 and 5.

We have analyzed, for the first time, the atomistic level structure of the liquid-liquid like interface lying beneath the real liquid surface of imidazolium-based RTILs and separates the bulk ionic liquid from the overlying hydrocarbon layer, formed by the outmost cation alkyl chains. This 'ionic surface' shows much stronger structural similarity in systems corresponding to cation alkyl chains of different lengths than the real liquid surface, the residual differences being traced back to the effect of the cation chain length on the surface orientation of the imidazolium ring. The aforementioned structural robustness of this 'ionic surface' puts forward the view that the free surface of imidazolium-based RTILs, covered by a thin oily layer of hydrocarbon chains, can indeed be regarded as the combination of a liquid-liquid like and a liquid-vapor like interface, separating the ionic system from the oily surface layer and this layer from the vapor phase, respectively.

While experimental studies unequivocally show the presence of an alkyl layer at the surface of imidazolium-based RTILs,[50-52] details regarding the precise arrangement and orientation of individual ions are less consensual.[50] Our simulation results support experimental interpretations based on the presence of a densely-packed ionic layer located just beneath the apolar layer, with the ionic layer being only partially accessible from the vapor phase.[13,51,55,56] Further, the independence of the properties of this apolar layer on the cation chain length had not been demonstrated before. Our finding could also be helpful in resolving seeming contradictions between the conclusions of various experiments, keeping in mind that different surface-sensitive experimental techniques might probe either of the above two interfaces, or even both of them. As an example, while in sum frequency generation (SFG) spectroscopy measurements, predominantly probing the C-H vibration modes at the liquid surface, a marked decrease of the liquid density was found at the surface,[13] a roughly

18% increase of the liquid phase density was found by X-ray reflectivity in the 6-7 Å wide surface layer, which includes both of these interfaces.[9]

The extent of coverage of the surface by hydrophobic groups can be controlled by changing the alkyl chain length, and this has concomitant effects on the surface tension; for example, it is known experimentally that the surface tension of imidazolium ILs decreases with chain length and approaches values typical of alkane surfaces.[57,58] However, our results show that such changes have minimal effect on the underlying ionic surface, which remains a densely packed polar "barrier" separating the vapor phase from the bulk liquid. These observations are of significant relevance for studies of molecule/ion transfer across RTIL interfaces, which are important in many practical applications of such liquids.

Supporting Information. Figures showing the structure of the ions considered, layerwise atomic composition of the systems studied with respect to the real liquid surface, atomic and charge density profiles not normalized by the bulk values.

Acknowledgements

This work has been supported by the Hungarian NKFIH Foundation under Project No. 142258.

References

(1) *Ionic Liquids in Synthesis*; Wasserscheid, P.; Welton, T., Eds.; Wiley-VCH: Weinheim, 2008.

(2) Welton, T. Room-Temperature Ionic Liquids. Solvents for Synthesis and Catalysis. *Chem. Rev.* **1999,** *99,* 2071-2084.

(3) Hapiot, P.; Lagrost, C. Electrochemical Reactivity in Room-Temperature Ionic Liquids. *Chem. Rev.* **2008,** *108,* 2238-2264.

(4) Avila, J.; Corsini, C.; Correa, C. M.; Rosenthal, M.; Pádua, A.; Costa Gomes, M. C. Porous Ionic Liquids Go Green. *ACS Nano* **2023,** *17,* 19508-19513.

(5) Blanchard, L. A.; Hancu, D.; Beckman, E. J.; Brennecke, J. F. Green Processing Using Ionic Liquids and CO_2. *Nature* **1999,** *399,* 28-29.

(6) Anthony, J. L.; Aki, S. N.; Maginn, E. J.; Brennecke, J. F. Feasibility of Using Ionic Liquids for Carbon Dioxide Capture. *Int. J. Environ. Technol. Manage.* **2004,** *4*, 105-115.

(7) Noorani, N.; Mehrdad, A. Solubility of Carbon Dioxide in Some Imidazolium and Pyridinium-Based Ionic Liquids and Correlation with NRTL Model. *Aus. J. Chem.* **2022,** *75*, 353-361.

(8) Iimori, T.; Iwahashi, T.; Ishii, H.; Seki, K.; Ouchi, Y.; Ozawa, R.; Hamaguchi, H.; Kim, D. Orientational Ordering of Alkyl Chain at the Air/Liquid Interface of Ionic Liquids Studied by Sum Frequency Vibrational Spectroscopy. *Chem. Phys. Letters* **2004,** *389*, 321-326.

(9) Sloutskin, E.; Ocko, B. M.; Tamam, L.; Kuzmenko, I.; Gog, T.; Deutsch. M. Surface Layering in Ionic Liquids: An X-ray Reflectivity Study. *J. Am. Chem. Soc.* **2005,** *127*, 7796-7804.

(10) Vargara-Gutierrey, M. C.; Webster, J. R. P. Surface Ordering of Amphiphilic Ionic Liquids. *Langmuir* **2004,** *20*, 309-312.

(11) Santos, C. S.; Rivera-Rubero, S.; Dibrov, S.; Baldelli, S. Ions at the Surface of a Room-Temperature Ionic Liquid. *J. Phys. Chem. C* **2007,** *111*, 7682-7691.

(12) Santos, C. S.; Baldelli, S. Gas−Liquid Interface of Hydrophobic and Hydrophilic Room-Temperature Ionic Liquids and Benzene: Sum Frequency Generation and Surface Tension Studies. *J. Phys. Chem. C* **2008,** *112*, 11459-11467.

(13) Jeon, Y.; Sung, J.; Bu, W.; Vaknin, D.; Ouchi, Y.; Kim, D. Interfacial Restructuring of Ionic Liquids Determined by Sum-Frequency Generation Spectroscopy and X-Ray Reflectivity. *J. Phys. Chem. C* **2008,** *112*, 19649-19654.

(14) Chevrot, G.; Schurhammer, R.; Wipff, G. Molecular Dynamics Simulation of the Aqueous Interface with the [BMI][PF_6] Ionic Liquid: Comparison of Different Solvent Models. *Phys. Chem. Chem. Phys*. **2006,** *8*, 4166-4174.

(15) Sarangi, S. S.; Raju, S. G.; Balasubramanian, S. Molecular Dynamics Simulations of Ionic Liquid–Vapour Interfaces: Effect of Cation Symmetry on Structure at the Interface. *Phys. Chem. Chem. Phys.* **2011,** *13*, 2714–2722.

(16) Hantal, G.; Cordeiro, M. N. D. S.; Jorge, M. What Does an Ionic Liquid Surface Really Look Like? Unprecedented Details from Molecular Simulations. *Phys. Chem. Chem. Phys.* **2011,** *1*3, 21230-21232.

(17) Lísal, M.; Posel, Z.; Izák, P. Air–Liquid Interfaces of Imidazolium-Based [TF_2N^-] Ionic Liquids: Insight from Molecular Dynamics Simulations. *Phys. Chem. Chem. Phys.* **2012,** *14*, 5164-5177.

(18) Hantal, G.; Voroshylova, I.; Cordeiro, M. N. D. S.; Jorge, M. A Systematic Molecular Simulation Study of Ionic Liquid Surfaces Using Intrinsic Analysis Methods. *Phys. Chem. Chem. Phys.* **2012,** *14*, 5200-5213.

(19) Paredes, X.; Fernández, J.; Pádua, A. A. H.; Malfreyt, P.; Malberg, F.; Kirchner, B.; Pensado, A. S. Using Molecular Simulation to Understand the Structure of $[C_2C_1im]^+$–Alkylsulfate Ionic Liquids: Bulk and Liquid–Vapor Interfaces. *J. Phys. Chem. B* **2012,** *116*, 14159–14170.

(20) Lísal, M.; Izák, P. Molecular Dynamics Simulations of n-Hexane at 1-Butyl-3-Methylimidazolium bis(Trifluoromethylsulfonyl) Imide Interface. *J. Chem. Phys.* **2013,** *139*, 014704.

(21) Paredes, X.; Fernández, J.; Pádua, A. A. H.; Malfreyt, P.; Malberg, F. Kirchner, B.; Pensado, A. S. Bulk and Liquid-Vapor Interface of Pyrrolidinum-Based Ionic Liquids: A Molecular Simulation Study. *J. Phys. Chem. B* **2014,** *118*, 731-742.

(22) Malberg, F.; Hollóczki, O.; Thomas, M. Kirchner, B. En Route Formation of Ion Pairs at the Ionis Liquid-Vacuum Interface. *Struct. Chem.* **2015,** *26*, 1343-1349.

(23) Hantal, G.; Sega, M.; Kantorovich, S.; Schröder, C.; Jorge, M. Intrinsic Structure of the Interface of Partially Miscible Fluids: An Application to Ionic Liquids. *J. Phys. Chem. C.* **2015,** *119*, 28448-28461.

(24) Lapshin, D. N.; Jorge, M.; Campbell, E. E. B.; Sarkisov, L. On Competitive Gas Adsorption and Absorption Phenomena in Thin Films of Ionic Liquids. *J. Mater. Chem. A* **2020,** *8*, 11781-11799.

(25) Tóth Ugyonka, H.; Hantal, G.; Szilágyi, I.; Idrissi, A.; Jorge, M.; Jedlovszky, P. Spatial Organization of the Ions at the Free Surface of Imidazolium-Based Ionic Liquids. *J. Coll. Interface Sci.* **2024,** *676*, 989-1000.

(26) Tóth Ugyonka, H.; Hantal, G.; Szilágyi, I.; Idrissi, A.; Jorge, M.; Jedlovszky, P. Single Particle Dynamics at the Free Surface of Imidazolium-Based Ionic Liquids. *J. Phys. Chem. B* **2025,** *129*, 579-591.

(27) Palunas, K.; Sprenger, K. G.; Weidner, T.; Pfaendtner, J. Effect of an Ionic Liquid/Air Interface on the Structure and Dynamics of Amphiphilic Peptides. *J. Mol. Liquids* **2017,** *236*, 404-413.

(28) Ghahari, A.; Raissi, H. Ionic Liquids and Graphene: The Ultimate Combination for High-Performance Supercapacitors. *J. Mol. Liquids* **2024,** *401*, 124523.

(29) Nada, H.; Unknown Crystal-Like Phases Formed in an Imidazolium Ionic Liquid: A Metadynamics Simulation Study. *J. Chem. Phys.* **2024,** 160, 204501.

(30) Rowlinson, J. S.; Widom, B. *Molecular Theory of Capillarity*; Dover Publications: Mineola, 2002.

(31) Chacón, E.; Tarazona, P. Intrinsic Profiles Beyond the Capillary Wave Theory: A Monte Carlo Study. *Phys Rev. Letters* **2003,** *91*, 166103.

(32) Chowdhary, J.; Ladanyi, B. M. Water-Hydrocarbon Interfaces: Effect of Hydrocarbon Branching on Interfacial Structure. *J. Phys. Chem. B.* **2006,** *110*, 15442-15453.

(33) Jorge, M.; Cordeiro, M. N. D. S. Intrinsic Structure and Dynamics of the Water/Nitrobenzene Interface. *J. Phys. Chem. C.* **2007,** *111*, 17612-17626.

(34) Pártay, L. B.; Hantal, G.; Jedlovszky, P.; Vincze, Á.; Horvai, G. A New Method for Determining the Interfacial Molecules and Characterizing the Surface Roughness in Computer Simulations. Application to the Liquid–Vapor Interface of Water. *J. Comp. Chem.* **2008,** *29*, 945-956.

(35) Jorge, M.; Jedlovszky, P.; Cordeiro, M. N. D. S. A Critical Assessment of Methods for the Intrinsic Analysis of Liquid Interfaces. 1. Surface Site Distributions. *J. Phys. Chem. C.* **2010,** *114*, 11169-11179.

(36) Wilard, A. P.; Chandler, D. Instantaneous Liquid Interfaces. *J. Phys. Chem. B.* **2010,** *114*, 1954-1958.

(37) Sega, M.; Kantorovich, S.; Jedlovszky, P; Jorge, M. The Generalized Identification of Truly Interfacial Molecules (ITIM) Algorithm for Nonplanar Interfaces. *J. Chem. Phys.* **2013,** *138*, 044110.

(38) Pártay, L. B.; Horvai, G.; Jedlovszky, P. Temperature and Pressure Dependence of the Properties of the Liquid-Liquid Interface. A Computer Simulation and Identification of the Truly Interfacial Molecules Investigation of the Water-Benzene System. *J. Phys. Chem. C.* **2010,** *114*, 21681-21693.

(39) Sega, M.; Horvai, G.; Jedlovszky, P. Microscopic Origin of the Surface Tension Anomaly of Water. *Langmuir* **2014,** *30*, 2969-2972.

(40) Sega, M.; Horvai, G.; Jedlovszky, P. Two-Dimensional Percolation at the Free Water Surface and its Relation with the Surface Tension Anomaly of Water. *J. Chem. Phys.* **2014,** *141*, 054707.

(41) Abraham, M. J.; Murtola, T.; Schulz, R.; Páll, S.; Smith, J. C.; Hess, B.; Lindahl, E. GROMACS: High Performance Molecular Simulations Through Multi-Level Parallelism from Laptops to Supercomputers. *SoftwareX* **2015,** *1-2*, 19-25.

(42) Sambasivarao, S.V.; Acevedo, O. Development of OPLS-AA Force Field Parameters for 68 Unique Ionic Liquids, *J. Chem. Theory Comput.* **2009,** *5*, 1038-1050.

(43) Doherty, B.; Zhong, X.; Gathiaka, S.; Li, B.; Acevedo, O. Revisiting OPLS Force Field Parameters for Ionic Liquid Simulations. *J. Chem. Theory Comput.* **2017,** *13*, 6131-6145.

(44) Essman, U.; Perera, L.; Berkowitz, M. L.; Darden, T.; Lee, H.; Pedersen, L. G. A Smooth Particle Mesh Ewald Method. *J. Chem. Phys.* **1995,** *103*, 8577-8594.

(45) in't Veld, P. J.; Ismail, A. E.; Grest, G. S. Application of Ewald Summations to Long–Range Dispersion Forces. *J. Chem. Phys*. **2007,** *127*, 144711.

(46) Bussi, G.; Donadio, D.; Parrinello, M. Canonical Sampling through Velocity Rescaling. *J. Chem. Phys.* **2007,** *126*, 014101.

(47) URL: https://github.com/Marcello-Sega/pytim (last accessed: November 20, 2023).

(48) Sega, M.; Hantal, G.; Fábián, B.; Jedlovszky, P. Pytim: A Python Package for the Interfacial Analysis of Molecular Simulations. *J. Comp. Chem.*, **2018,** *39*, 2118-2125.

(49) Sega, M.; Fábián, B.; Jedlovszky, P. Layer-by-Layer and Intrinsic Analysis of Molecular and Thermodynamic Properties Across Soft Interfaces. *J. Chem. Phys.* **2015,** 143, 114709.

(50) Santos, C. S.; Baldelli, S. Gas-Liquid Interface of Room-Temperature Ionic Liquids. *Chem. Soc. Rev.* **2010,** *39*, 2136-2145.

(51) Maier, F.; Cremer, T.; Kolbeck, C.; Lovelock, K. R. J.; Paape, N.; Schulz, P. S.; Wasserscheid, P.; Steinrück, H. P. Insight into the Surface Composition and Enrichment Effects of Ionic Liquids and Ionic Liquid Mixtures. *Phys. Chem. Chem. Phys.* **2010,** *12*, 1905-1915.

(52) Tesa-Serrate, M. A.; Marshall, B. C.; Smoll, Jr.; E. J.; Purcell, S. M.; Costen, M. L.; Slattery, J. M.; Minton, T. K.; McKendrick, K. G. Ionic Liquid–Vacuum Interfaces Probed by Reactive Atom Scattering: Influence of Alkyl Chain Length and Anion Volume. *J. Phys. Chem. C* **2015,** *119*, 5491-5505.

(53) Ester, M.; Kriegel, H. P.; Sander, J.; Xu, X. A Density-Based Algorithm for Discovering Clusters in Large Spatial Databases with Noise; In: *Proceedings of the Second International Conference on Knowledge Discovery and Data Mining (KDD-*

96); Simoudis, E.; Han, J.; Fayyad, U. M., Eds.; AAAI Press: Washington, D. C., 1996, pp. 226-231.

(54) Ridings, C.; Lockett, V.; Andersson, G. Effect of the Aliphatic Chain Length on Electrical Double Layer Formation at the Liquid/Vacuum Interface in the [$C_n$mim][BF_4] Ionic Liquid Series. *Phys. Chem. Chem. Phys.* **2011,** *13*, 17177-17184.

(55) Lovelock, K. R. J.; Kolbeck, C.; Cremer, T.; Paape, N.; Schulz, P. S.; Wasserscheid, P.; Maier, F.; Steinrück, H. P. Influence of Different Substituents on the Surface Composition of Ionic Liquids Studied Using ARXPS. *J. Phys. Chem. B* **2009,** *113*, 2854-2864.

(56) Kolbeck, C.; Cremer, T.; Lovelock, K. R. J.; Paape, N.; Schulz, P. S.; Wasserscheid, P.; Maier, F.; Steinrück, H. P. Influence of Different Anions on the Surface Composition of Ionic Liquids Studied Using ARXPS. *J. Phys. Chem. B* **2009,** *113*, 8682-8688.

(57) Kolbeck, C.; Lehmann, J.; Lovelock, K. R. J.; Cremer, T.; Paape, N.; Wasserscheid, P.; Fröba, A. P.; Maier, F.; Steinrück, H. P. Density and Surface Tension of Ionic Liquids. *J. Phys. Chem. B* **2010,** *114*, 17025-17036.

(58) Steinrück, H. P. Recent Developments in the Study of Ionic Liquid Interfaces Using X-Ray Photoelectron Spectroscopy and Potential Future Directions. *Phys. Chem. Chem. Phys.* **2012,** *14*, 5010-5029.

Figure legends

Figure 1. Equilibrium snapshot of the surface portion of [bmim][PF_6] at 298K, illustrating the difference between the liquid surface and ionic surface of the system.

Figure 2. Mole fraction of the cations in the first four molecular layers beneath (a) the ionic, and (b) the real liquid surface of [mmim][PF_6] (black), [bmim][PF_6] (red) and [omim][PF_6] (blue) at 298K (top) and 398K (bottom).

Figure 3. (a) Mole fraction of atoms belonging to the anions (black), imidazolium ring (red), methyl group (green) and alkyl trunk CH_2 group (blue) in the first ten atomic layers beneath the ionic surface at 298K (top) and 398K (bottom). Data corresponding to the two equivalent methyl side groups of the $mmim^+$ cation are shown by khaki color. (b) Charge surface density in the first ten atomic layers beneath the ionic surface (top) and real liquid surface (bottom) in [mmim][PF_6] (squares), [bmim][PF_6] (circles), and [omim][PF_6] (diamonds).

Figure 4. Number density profile of the cation C atoms pertaining to the imidazolium ring, bound to both N atoms (black), methyl group (red), and alkyl trunk CH_2 group (blue), and anion P (orange) and F (green) atoms relative to the intrinsic ionic surface, normalized by the bulk liquid phase values. The profile corresponding to the two equivalent methyl groups of $mmim^+$ is shown by purple color. The cation C atoms considered are marked by asterisks in Fig. S1 of SI. Lines: [mmim][PF_6], full circles: [bmim][PF_6], open circles: [omim][PF_6]. Arrows indicate the Dirac delta contribution of the first layer atoms.

Figure 5. Left: charge density profile relative to the intrinsic ionic surface for [mmim][PF_6] (black), [bmim][PF_6] (red), and [omim][PF_6] (blue). Right: cation (brown) and anion (green) contributions to the intrinsic charge density profile, normalized by the corresponding bulk liquid phase values. Lines: [mmim][PF_6], full circles: [bmim][PF_6], open circles: [omim][PF_6]. Top and bottom panels show the profiles obtained at 298K and 398K, respectively. Scales refer to the panels at the respective sides. Arrows indicate the Dirac delta contribution coming from the first layer atoms.

Figure 6. (a) Number density profile of the anion P (orange) and F (green) atoms with respect to the intrinsic ionic surface, as obtained in [omim][PF_6] at 398 K by filtering out the charged moieties 'dissolved' into the surface hydrocarbon layer using DBSCAN with search radii of 4.5 Å (filled triangles) and 6.0 Å (open down triangles), as well as without DBSCAN (lines). The Dirac delta contribution of the first layer atoms is indicated by the arrow. (b) Cosine distribution of the angle γ, formed by the **NN** vector of the imidazolium ring (see Fig. S1 of the SI) and the macroscopic surface normal vector, **X**, pointing from the liquid to the vapor phase, as obtained in the first molecular layer of [mmim][PF_6] (black squares), [bmim][PF_6] (red circles), and [omim][PF_6] (blue diamonds) at 398 K.

Figure 1.

Tóth Ugyonka et al.

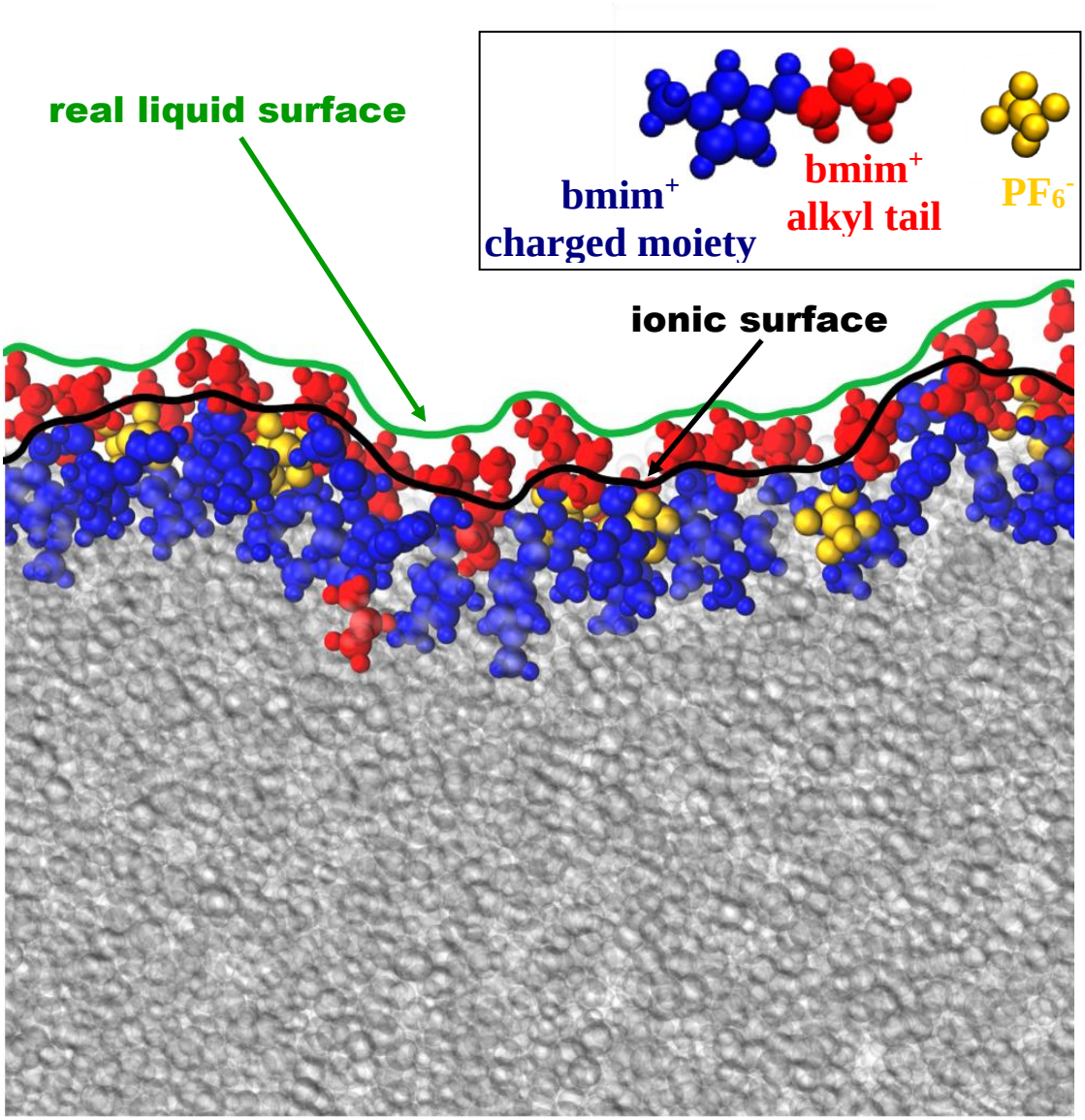

Figure 2.

Tóth Ugyonka et al.

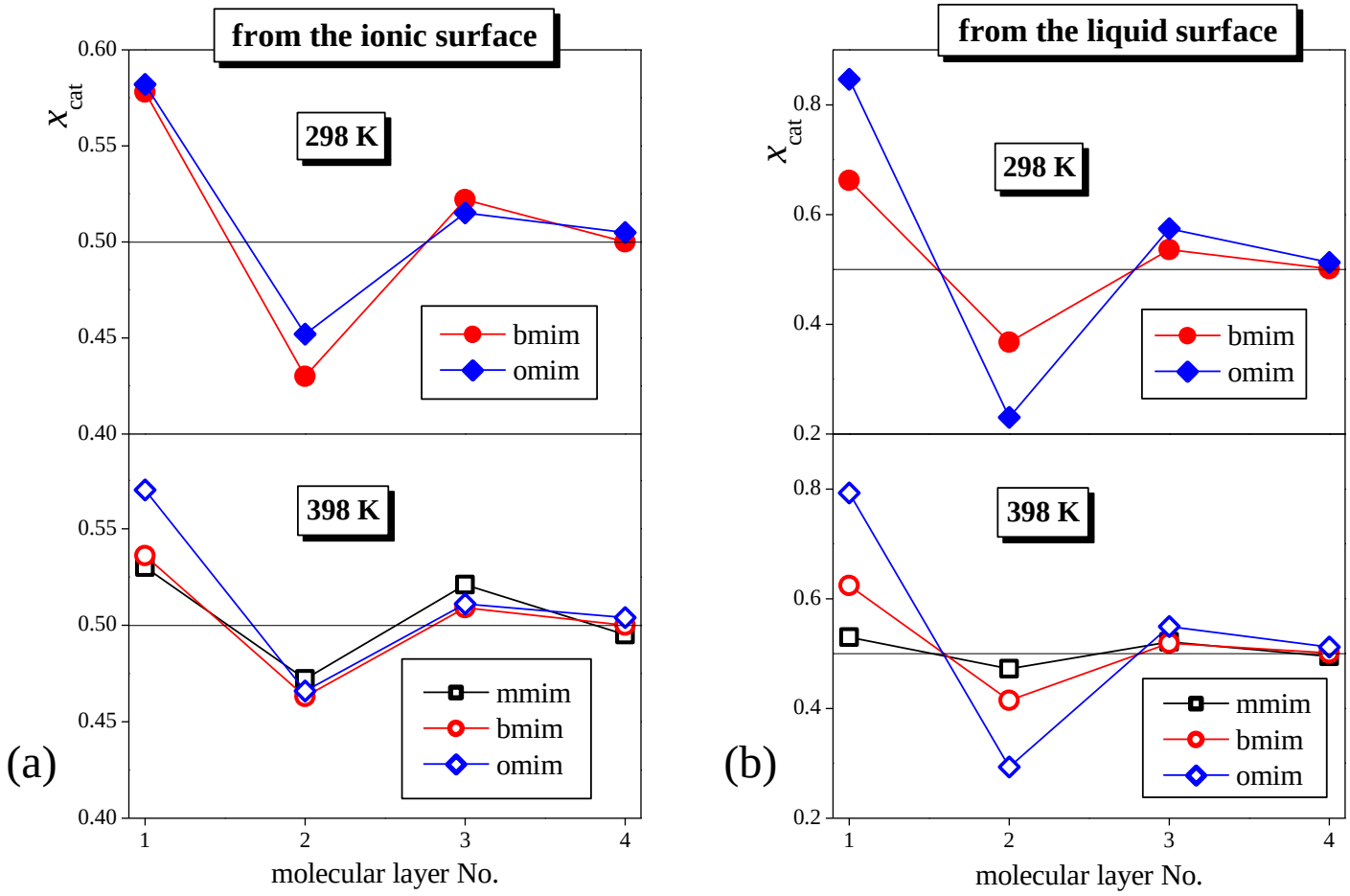

Figure 3.

Tóth Ugyonka et al.

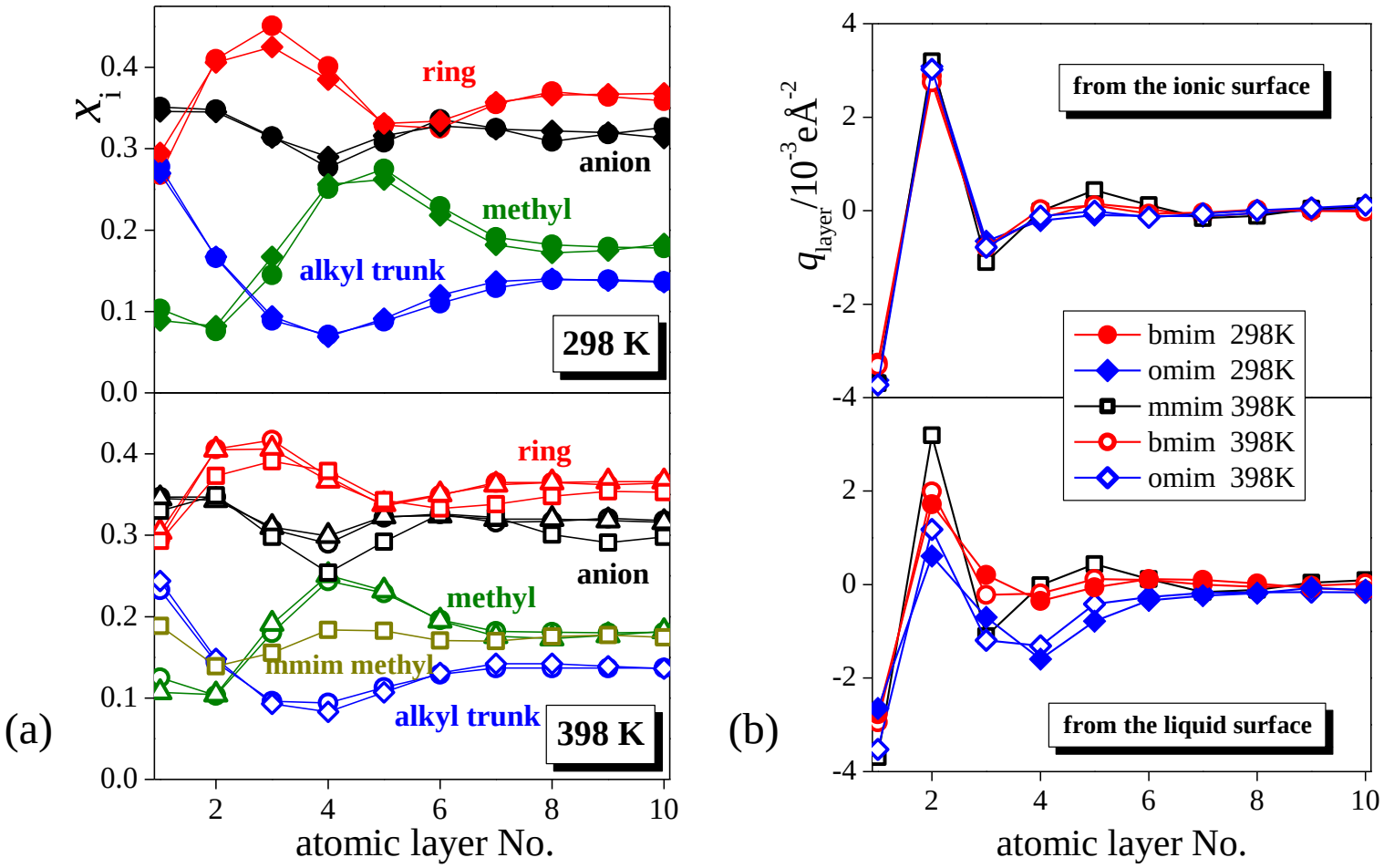

Figure 4.

Tóth Ugyonka et al.

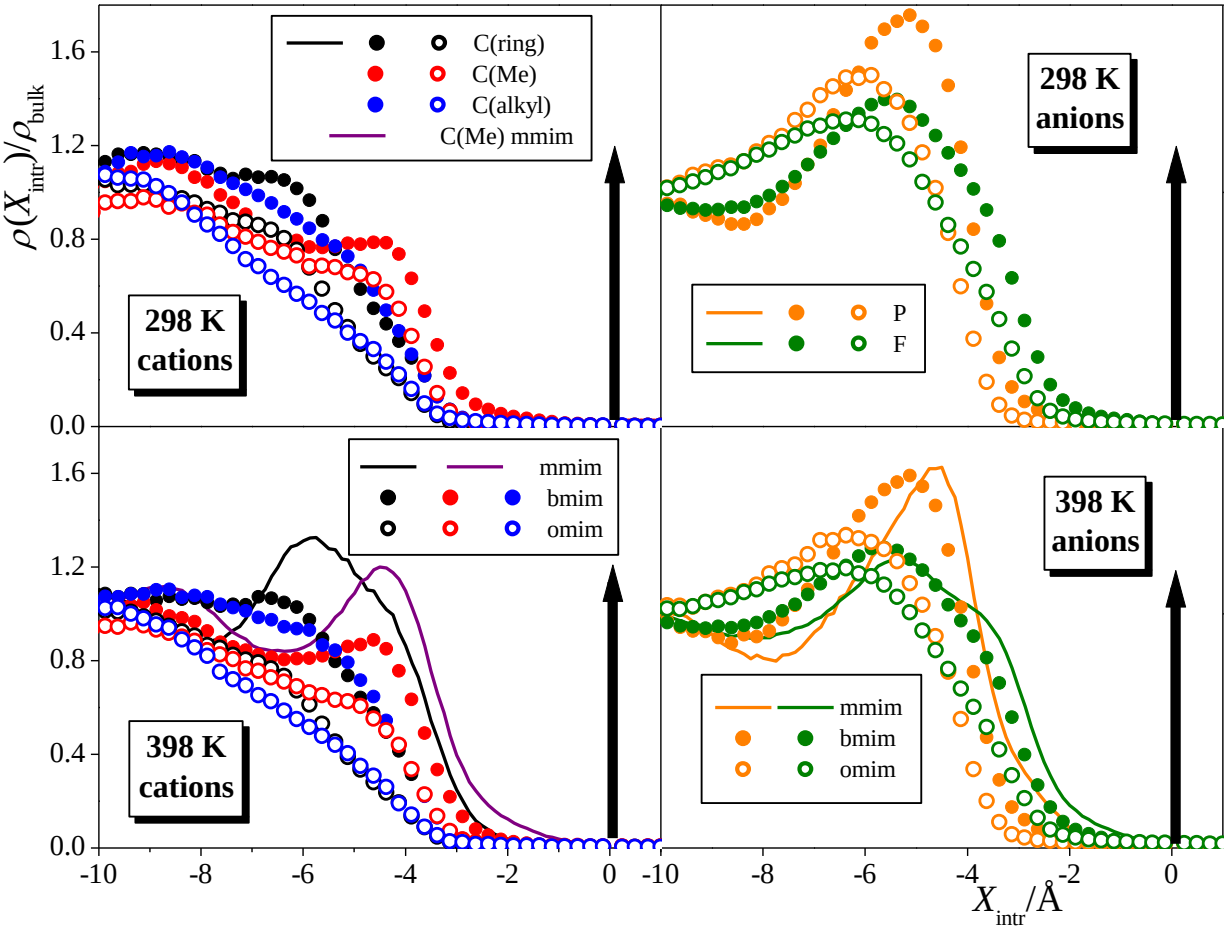

Figure 5.

Tóth Ugyonka et al.

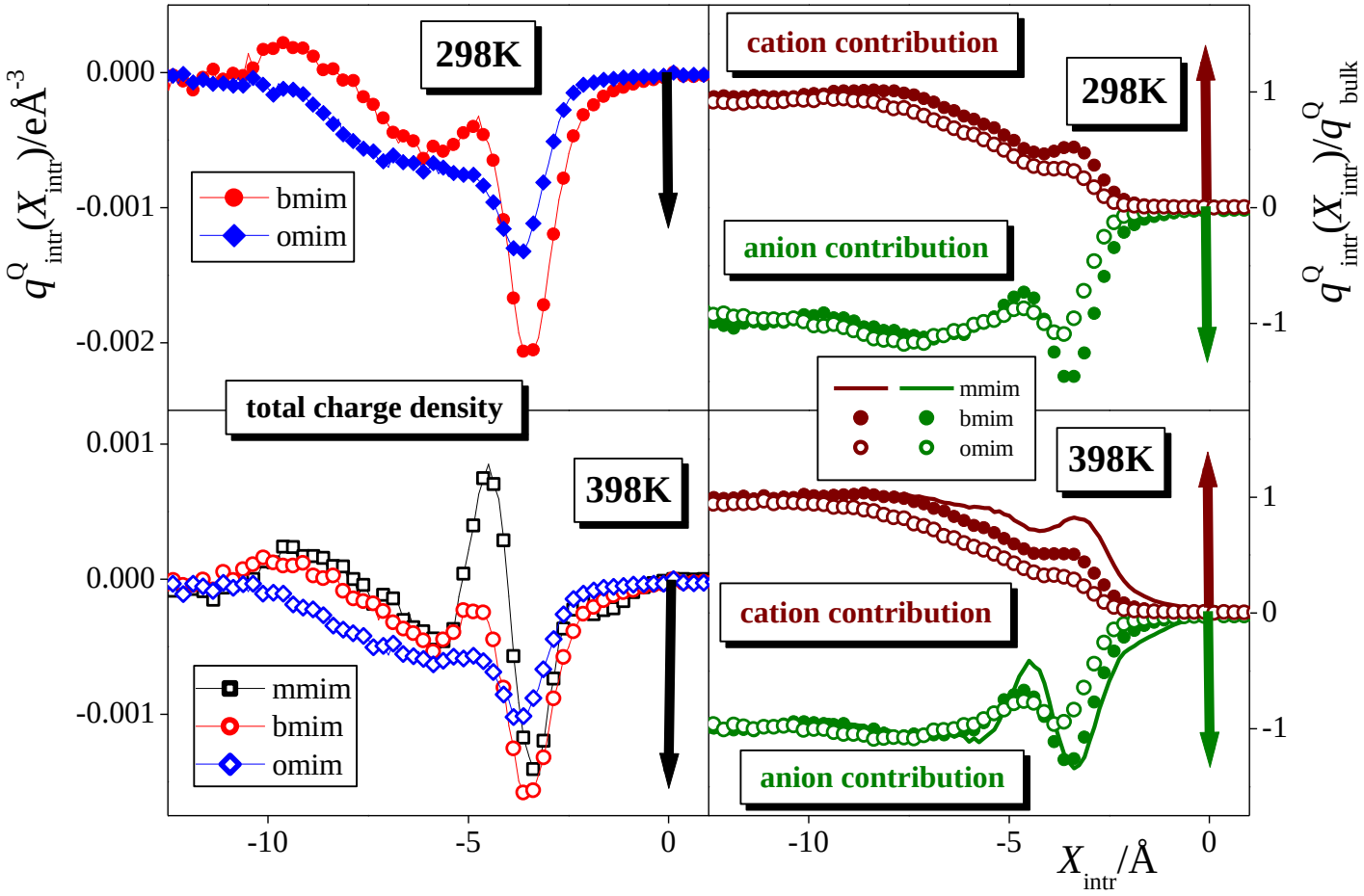

Figure 6.

Tóth Ugyonka et al.

(a)

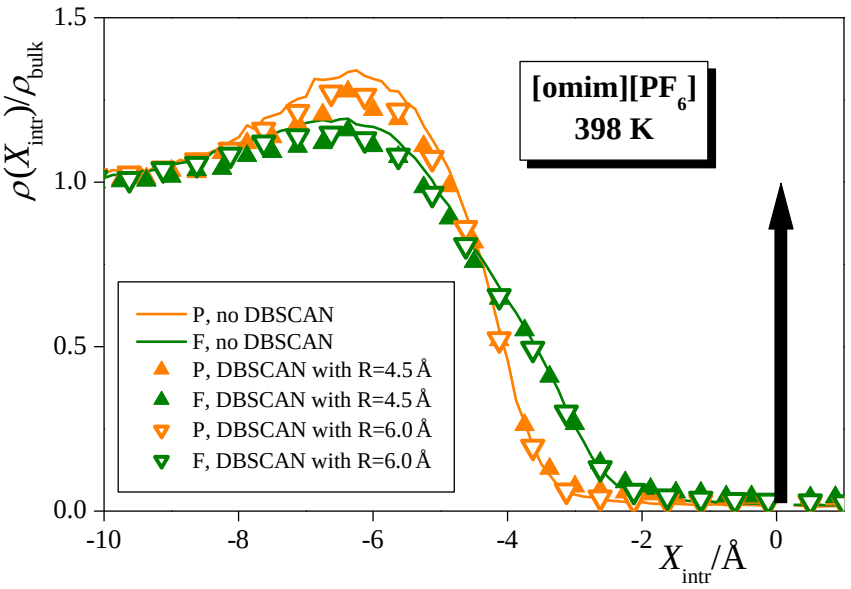

(b)

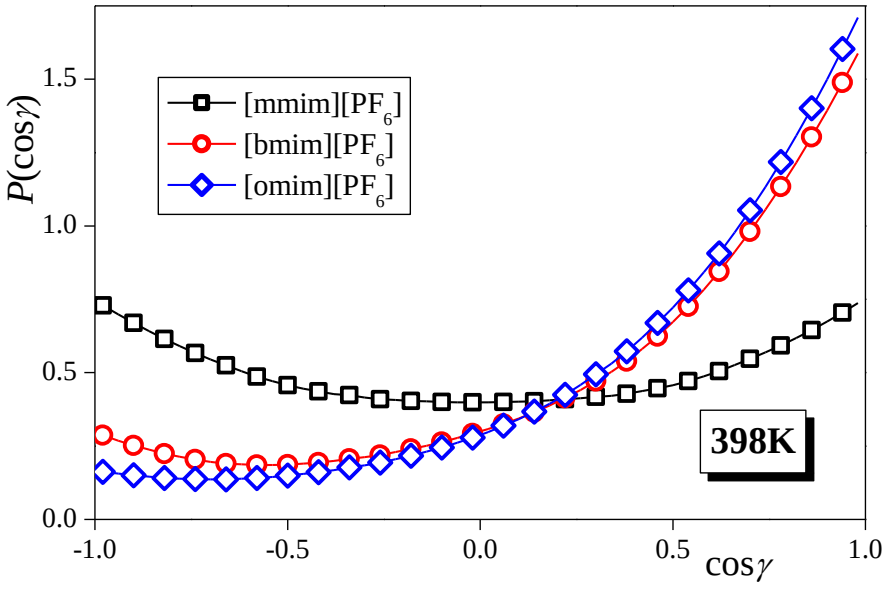

TOC Graphic: